Original Article

Toxicopathological Effects of Brodifacoum in Rats Following Secondary Exposure

Mohammed A Mahdi Al-Kubaisi[1], Raghad N Al-Saadi[1], Siti Nur F Muhsain[2]

1. Department of Pathology and Poultry Diseases, College of Veterinary Medicine, University of Baghdad, Baghdad, Iraq.
2. Faculty of Pharmacy, Universiti Teknologi MARA, Bertam Campus, Cawangan Pulau Pinang, Malaysia.

Use your device to scan and read the article online

How to Cite This Article Al-Kubaisi, MAM., Al-Saadi, RN., & Muhsain, SNF. (2026). Toxicopathological Effects of Brodifacoum in Rats Following Secondary Exposure. *Iranian Journal of Veterinary Medicine, 20*(3), 587-604. http://dx.doi.org/10.32598/ijvm.20.3.1005961

http://dx.doi.org/10.32598/ijvm.20.3.1005961

ABSTRACT

Background: Brodifacoum is a highly lethal 4-hydroxycoumarin anticoagulant rodenticide that acts as a vitamin K antagonist. Its lipophilic nature enables long-term retention in tissues allowing predators and scavengers to become exposed through contaminated prey. Despite its widespread use its toxicopathological effects remain insufficiently defined.

Objectives: This study aimed to investigate the toxicopathological effects of brodifacoum using male rats following secondary exposure through contaminated liver homogenate.

Methods: Ninety rats were randomly divided into four groups: group G1 received brodifacoum bait for 24 to 48 hours (primary toxicity), group G2 served as an untreated control, group G3 received an untreated liver homogenate from G2 to be used as a secondary control and group G4 received a liver homogenate contaminated with brodifacoum from G1 (secondary toxicity). Hepatic residues were determined using high-performance liquid chromatography (HPLC), and cytochrome P450 (CYP450) levels were measured using an enzyme-linked immunosorbent assay (ELISA) kit. Gross examination, hemorrhagic scoring, and histopathological examinations were conducted on major organs.

Results: HPLC analysis confirmed that brodifacoum significantly accumulated in the liver. G4 showed around a fivefold higher residue level (17.87±0.11 µg/g) compared with G1 (3.53±0.49 µg/g). Hepatic CYP450 content showed a 1.8-fold increase in G4 relative to G3 ($P<0.0001$). Gross and microscopic examinations revealed marked hemorrhagic and degenerative changes, most prominent in the lungs, liver, and kidneys in G4.

Conclusion: The results of the current study support the use of male rats as a model to evaluate the toxicopathological effects of brodifacoum following secondary exposure.

Keywords: Anticoagulant rodenticide (ARs), Secondary toxicity, Cytochrome P450 (CYP450), Hepatic bioaccumulation, Hemorrhagic score

Article info:
Received: 15 Jan 2025
Accepted: 29 Feb 2026
Publish: 01 May 2026

*** Corresponding Author:**
Mohammed A Mahdi Al-Kubaisi
Address: *Department of Pathology and Poultry Diseases, College of Veterinary Medicine, University of Baghdad, Baghdad, Iraq.*
E-mail: *mohammed.abdulsatar1307a@covm.uobaghdad.edu.iq*

Introduction

Anticoagulant rodenticides (ARs) are among the most widely used pesticides for rodent population control and to mitigate their impact in urban and agricultural environments (Soh et al., 2022; Valverde et al., 2021). These compounds act by inhibiting vitamin K-dependent clotting factors II, VII, IX, and X, leading to delayed but fatal hemorrhage in rodents following the ingestion of a lethal dose (Buckley et al., 2023; Priya et al., 2025). ARs are classified into first-generation (FGARs), intermediate-generation (IGARs), and second-generation ARs (SGARs) based on their potency and half-life (Rattner & Harvey, 2021). FGARs, such as warfarin and coumachlor, are less potent and have a shorter half-life compared to later generations, requiring rodents to eat the bait over several feedings to receive a lethal dose (Buckley et al., 2023). SGARs, also known as "superwarfarins", such as brodifacoum, bromadiolone, and difenacoum, are more potent and have prolonged persistence and toxicity, often attaining lethality with a single feeding (Scammell et al., 2024). IGARs, such as chlorophacinone and pindone, fall between FGARs and SGARs in potency and persistence and resemble FGARs in their mode of action (Rattner & Harvey, 2021). The practical advantage of ARs is their delayed onset, on average spanning four to nine days, which allows rodents to repeat consumption the bait before experiencing symptoms. This allows overcome "the bait shyness" when rodents associate the consumption of bait to consequences and develop avoidance behaviors (Riegraf et al., 2022; Shahwar et al., 2024). While this feature enhances AR effectiveness, it also increases the risk of secondary poisoning (Murray, 2020). Non-target species, including predators and scavengers, are at risk through primary exposure (direct consumption of bait) or secondary exposure (consumption of poisoned rodents). During the latent period, poisoned rodents spend more time in open areas in a lethargic state and are more susceptible to predation, further increasing secondary exposure risks (Buckley et al., 2023; Caliani et al., 2023).

Among the superwarfarins, brodifacoum is one of the most commonly used compounds (Ragab et al., 2019). It can be lethal after a single ingestion, making it a preferred choice in pest control programs (Rattner et al., 2019; Stading et al., 2020). However, brodifacoum has a long biological half-life and remains in liver tissues for months. This prolonged persistence in biological systems poses significant ecological risks and may lead to increased bioaccumulation in target and non-target species (Hernández-Moreno et al., 2013; Scammell et al., 2024). Predators and scavengers, such as birds of prey and carnivorous mammals, are usually vulnerable through secondary exposure. It has been suggested that such bioaccumulation can be transferred through higher trophic levels, potentially disrupting food webs and contributing to population declines among sensitive species (Scammell et al., 2024). Several studies have documented brodifacoum toxic effects, including disruption of the coagulation system and hemorrhagic events, in particular secondary poisoning cases (Rattner et al., 2019). Despite these data, notable gaps remain in understanding the metabolic pathways of brodifacoum, particularly the role of cytochrome P450 (CYP450) enzymes in its detoxification, as well as the histopathological changes that occur under secondary poisoning conditions (Rattner & Mastrota, 2017; Rached et al., 2020; Rubinstein et al., 2019). Besides other anthropogenic pollutants (Abduljalel & Al-Saadi, 2022; Ammar & Mohammed Mosleh, 2024; Shakir & Al-Saadi, 2025), the effects of long-term exposure to brodifacoum beyond hemostasis disruption remains insufficiently explored (Rattner & Mastrota, 2017; King & Tran, 2015; Ware et al., 2017).

The present study aimed to investigate the toxicopathological effects of brodifacoum following secondary exposure using a controlled mammalian model. This approach, utilizing Sprague-Dawley rats, provides a practical and ethically acceptable system for investigating secondary exposure dynamics and the basic toxicopathological effects of consuming contaminated tissue.

Materials and Methods

Chemicals and regents

Brodifacoum high-performance liquid chromatography (HPLC) grade with 98% purity (CAS NO. 56073-10-0) was purchased from Sigma Chemical Co. (St. Louis, USA). Commercial brodifacoum 0.005% paste was used to induce primary toxicity. A CYP450 ELISA (enzyme-linked immunosorbent assay) kit (SL0224Ra, assay kit) specific for rat liver samples was purchased from Sunlong Biotech Co. (Hangzhou, China). HPLC solvents used for HPLC analysis, including methanol, acetonitrile, acetone, and ammonium acetate, were of HPLC-grade (Merck, Germany).

Experimental animals

The experimental animal model used for this study was Sprague-Dawley rats. Ninety adult male rats about 12-14 weeks of age with an average weight of 200-250 g were

kept in a room at the animal house at the College of Veterinary Medicine, University of Baghdad. Animals were acclimatized for one week and provided with a standard rat pellet diet with water given ad libitum. The room temperature was maintained at 25-28 ˚C under a 12:12 h light-dark cycle throughout of the experiment.

Rats were randomly divided into four experimental group: two treatment groups and two corresponding control groups. The primary toxicity included group 1 (G1), in which 30 rats were fed on brodifacoum 0.005% paste bait, and group 2 (G2), in which 30 rats were fed on standard diet without any treatment. The secondary toxicity included group 3 (G3), in which 15 rats were fed on homogenized liver tissues (untreated liver tissues) collected from group G2 to serve as a negative control and group 4 (G4), where 15 rats were fed on homogenized liver tissues intoxicated with brodifacoum collected from G1.

Primary toxicity induction

Following an overnight fasting, rats in G1 were exposed to a commercially available brodifacoum bait containing 0.005% active ingredient. The bait was offered in a no-choice feeding setup, where each rat was provided with the toxic bait as the sole food source and allowed to consume it freely over a period of approximately 24 to 48 hours. Water was provided ad libitum during this period. Animals were observed for clinical signs of toxicity of brodifacoum, including lethargy, hemorrhage, and respiratory difficulty. Once clear signs of toxicity appeared, euthanasia was performed using an overdose of a mixture of ketamine and xylazine. Liver samples were collected for residual analysis and preparation of homogenized liver tissues, which were used later to induce the secondary toxicity experiment.

Secondary toxicity induction

To simulate secondary toxicity, liver tissues were collected from donor rats previously exposed to a commercial anticoagulant rodenticide containing 0.005% brodifacoum (G1) and from negative control rats (G2). The livers were sliced into small pieces and homogenized using a manual homogenizer after dilution with distilled water at a ratio of 1:10 (w/v). Homogenization was performed with approximately 15 strokes, which were sufficient to disrupt the tissue and achieve a uniform homogenate. The resulting homogenate was filtered through the sterile filter to remove large debris.

Each rat in G3 received 1 mL of the liver homogenate (1 mL / per animal / daily / for 4 weeks) prepared from G2 (negative control) rats via oral gavage. Similarly, rats in G4 received 1 mL of the liver homogenate (1 mL / per animal / daily / for 4 weeks) prepared from G1 (brodifacoum-exposed) rats.

Sample collection

At the end of both experiments, the rats were euthanized using overdose anesthesia (Mustafa & Jawad, 2024), and tissue samples were taken. Six representative liver samples were collected from each of the toxicity groups (primary and secondary) for the determination of brodifacoum concentration by HPLC. In the secondary toxicology groups, additional liver samples were collected, frozen in liquid nitrogen, and stored until CYP450 levels were analyzed.

For pathological assessment, the liver, kidney, and lung were grossly examined for hemorrhagic scores. Tissue samples from the liver, kidney, spleen, and lung were then fixed in 10% neutral buffered formalin for the evaluation of histopathological changes.

HPLC analysis of brodifacoum residue in the liver tissue

Liver samples from both toxic groups (primary and secondary) were processed for residue extraction. Approximately 0.5 g of the liver tissue was homogenized in 5 mL of a solvent mixture consisting of acetonitrile, acetone, and methanol in a ratio of 1:1:2 (v/v). The homogenate was placed on a mechanical shaker for 30 minutes. The extraction solvent was separated through filtration, then evaporated to dryness under reduced pressure using a rotary evaporator, and the resulting dried extracts were stored at −20 ˚C until analysis.

The concentrations of brodifacoum in the liver tissue were determined using HPLC with a SYKAM system (Germany). Chromatographic separation was established using a C18 column (25 cm × 4.6 mm). The mobile phase consisted of an isocratic mixture of acetonitrile and 0.1 M ammonium acetate buffer (pH 5.4) in a 70:30 (v/v) ratio, delivered at a flow rate 1 mL/min. Detection was performed with a UV detector set at 264 nm. Quantification of brodifacoum was performed using the external standard method, as described by Meiser (Meiser, 2005), by comparing the peak areas of the samples with those of standard brodifacoum solutions analyzed under identical chromatographic conditions.

CYP450 quantification via ELISA

Liver homogenates were prepared for the determination of CYP450 using a rat-specific ELISA kit (Sunlong Biotech, Cat. No. SL0224Ra, Hangzhou, China). The liver tissue was homogenized in phosphate-buffered saline (PBS, pH 7.4) on ice and centrifuged at 2,000–3,000 rpm for 20 min at 4 ˚C; the supernatant was collected for analysis. The assay was performed according to the manufacturer's protocol with minor adjustments. Briefly, 40 µL of sample dilution buffer and 10 µL of liver homogenate (1:5 dilution) were added per well, the plates were sealed, and incubated for 30 min at 37 ˚C. After washing five times with 1× wash buffer (prepared from the 30× concentrate), 50 µL of HRP-conjugated anti-CYP450 reagent was added to each well and incubated for 30 min at 37 ˚C, followed by 5 additional washes. Then, 50 µL of chromogen solution A and 50 µL of chromogen solution B were added and incubated for 15 min at 37 ˚C protected from light. The reaction was stopped with 50 µL of stop solution. Absorbance was measured at 450 nm within 15 min (the blank well was used for baseline correction). CYP450 concentrations were interpolated from a standard curve prepared with kit standards (assay range: 0.5–40 ng/mL; sensitivity: 0.1 ng/mL). The results were expressed in ng/mL. The control group (G3) served as the baseline for calculation.

Gross and histopathological examination

At the end of the secondary toxicity experiment (after four weeks of exposure), animals from both the control group (G3) and the secondary toxicity group (G4) were euthanized for postmortem examination. Each group was initially composed of 15 rats; however, due to early mortality in G4 prior to the scheduled necropsy, only 12 animals per group were available for complete gross and histopathological assessment. A systematic gross examination was conducted to evaluate macroscopic alterations in vital organs, particularly the liver, kidneys, and lungs. The severity of gross hemorrhagic lesions was assessed using a semi-quantitative scoring system adapted and modified from previous organ-based pathological studies (Kaewamatawong et al., 2011), as summarized in Table 1.

For histopathological examination, representative sections from secondary toxicity groups of the liver, kidney, spleen, and lungs were excised and fixed in 10% neutral buffered formalin for 48 hours. The samples were then dehydrated in graded ethanol, cleared in xylene, and embedded in paraffin. Sections of 5 µm thickness were achieved using a rotary microtome (Leica RM2125RT) and stained with hematoxylin and eosin (H&E) (Al-Saadi et al., 2025). The slides were then examined under a light microscope to determine any pathological alterations.

Statistical analysis

All data were analyzed using GraphPad Prism software, version 10.2.2. Values of quantitative data were expressed as Mean±SD, and differences between groups were analyzed using an unpaired student's t-test. Ordinal data were expressed as median [interquartile range, IQR] and analyzed using the Friedman test and Dunn's post hoc multiple comparison test. The significance threshold for all statistical analyses was set at $P<0.05$.

Results

Brodifacoum residue levels in the liver tissue

Brodifacoum chromatography showed a consistent retention time of 4.18 minutes (Figure 1A), which matched the peaks detected in both treatment groups (G1 and G4) (Figure 1B and C, respectively). No corresponding peaks were observed in the negative control group (G3) (Figure 1D). The mean hepatic concentration in the secondary toxicity group (G4) was 17.87±0.11 µg/g, which

Table 1. The semi-quantitative scoring system used to assess gross hemorrhagic lesions in major organs

Score	Description
0	No visible hemorrhage
1	Focal or petechial hemorrhages localized to a single area or limited to the organ surface
2	Hemorrhages affecting two or more distinct regions, such as lobes or tissue layers, are multifocal
3	Diffuse hemorrhage involving most of the organ surface or parenchyma
4	Confluent hemorrhage accompanied by organ swelling, dark discoloration, or rupture

Note: The scoring system ranges from 0 (no lesion) to 4 (severe hemorrhage).

Table 2. Concentrations of brodifacoum in the liver samples (µg)

Animal	Brodifacoum Concentrations in the Liver Samples (µg)	
	Primary Toxicity Group (G1)*	Secondary Toxicity Group (G4)*
1	3.45	18.25
2	3.85	20.14
3	3.78	16.99
4	3.25	17.49
5	3.65	16.9
6	3.22	17.44
Mean±SD	3.53±0.268	17.87±1.21*

*Significant difference (P<0.0001).

was significantly higher (P<0.0001) that in the primary toxicity group (G1), at 3.53±0.49 µg/g, representing an approximate five-fold increase (Table 2).

CYP450 levels

CYP450 levels were estimated by interpolating the absorbance values from the standard curve (Figure 2). The results revealed statistically significant elevation (P<0.0001) in CYP450 levels in the treatment group (G4), 17.34±1.08 ng/mL, compared to 9.64±2.72 ng/mL in the control group (G3) (Figure 3).

Clinical signs and anatomic location of hemorrhage associated with brodifacoum poisoning

Rats exposed to brodifacoum in the primary toxicity group (G1) exhibited clinical signs of toxicity, including lethargy, weakness, anorexia, dyspnea, reluctance to move, and ataxia, followed by death within 4–7 days. These symptoms were accompanied by multiple bleeding spots and subcutaneous hemorrhages distributed throughout the body (Figure 4). Rats in G4 that received the liver tissue contaminated with brodifacoum from G1 (following 4 weeks of the experiment) began to exhibit signs of toxicity like those observed in the primary group (G1) by the third week. In contrast, control groups (G2 and G3) showed no signs of toxicity during the experiment period.

Gross examination and hemorrhagic score

The severity of hemorrhagic lesions in the liver, kidney, and lung of G4 rats expressed as median (range; IQ25–IQ75), were 3 [2–4] for the liver, 2 [2–3] for the kidney, and 4 [3–4] for the lung. Statistical analysis using Friedman's test revealed a significant difference among organs in hemorrhagic scores within G4 rats (P=0.0001). Post hoc Dunn's multiple comparison test indicated that the lung had significantly higher hemorrhagic scores compared with the kidney (P=0.001), whereas differences between the liver and the other organs were not statistically significant (P>0.05). Table 3 illustrates the gross hemorrhagic scores of rats in G4.

Liver

The gross pathological appearance of the liver from the control group (G3) showed a normal appearance without any significant lesions (Figure 5A). The gross pathological appearance of the liver from G4 revealed severe congestion affecting several lobes (Figure 5B). Moreover, edematous liver parenchyma with a round edge was observed in other intoxicated animals (Figure

Table 3. Hemorrhage scoring for rats in group G4 (n=12, median [IQR])

Organ	Median [IQR]
Liver	3 [2–4]AB
Kidney	2 [2–3]A
Lung	4 [3–4]B

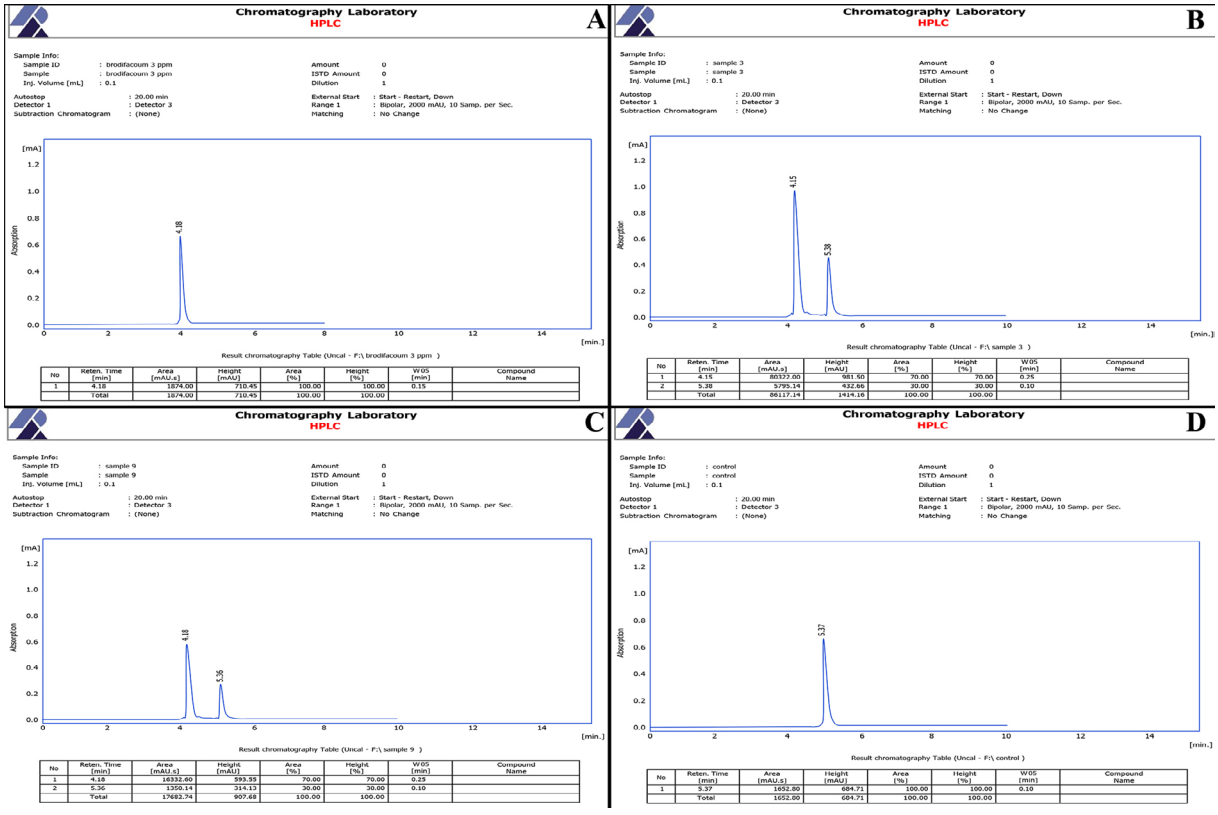

Figure 1. Chromatographic analysis of brodifacoum residues in rat liver sample

A) Chromatogram of the brodifacoum standard solution showing a retention time of 4.18 minutes, B) Chromatogram of brodifacoum residues in the liver of rats from group G4, C) Chromatogram of brodifacoum residues in the liver of rats from group G1, D) Chromatogram of rat liver from group G3 after four weeks of administration of control liver homogenate prepared from group G2, serving as a negative control

5C). Furthermore, some animals showed fatty liver and hepatomegaly (Figure 5D). According to the applied scoring system , the liver scored 2 [2-3], which suggests moderate to severe hemorrhagic involvement.

Kidney

The gross pathological examination of the kidney from the rat model in the G3 control group showed a normal kidney appearance (Figure 6A). In contrast, the cut surface of the kidney revealed multiple cortical and medullary hemorrhages (Figure 6C). Moreover, the kidneys in G4 that were secondarily intoxicated with brodifacoum following 4 weeks were enlarged and exhibited a subcapsular hematoma (Figure 6B). Moreover, the median hemorrhagic score observed in the kidney was 2 [2–3], reflecting moderate hemorrhagic injury.

Lungs

The lungs of G3 rats showed no evidence of hemorrhagic lesions (Figure 7A). Lungs from rats in G4 exhibited multifocal to coalescing dark red to black hemorrhagic patches affecting multiple lobes (massive pulmonary hemorrhage) (Figure 7B). Other animals in G4 revealed multiple hemorrhagic foci indicative of pulmonary hemorrhage and congestion (Figure 7C). Further, hemorrhagic scores for the lungs were consistently high, with a median score of 3 [2–4] in treated rats, indicating diffuse hemorrhage.

Histopathological examination

Liver

The control group (G3) showed normal hepatic architecture. The hepatic lobules were well-preserved, with hepatocytes arranged in cords radi-ating from the central vein, with no evidence of hemorrhage (Figure 8A). Liver sections from group G4 showed extensive hemorrhage and edema in the portal areas (Figure 8B). Microvascular degeneration of hepatocytes was observed, suggesting early cellular injury (Figure 8C). Moreover, focal

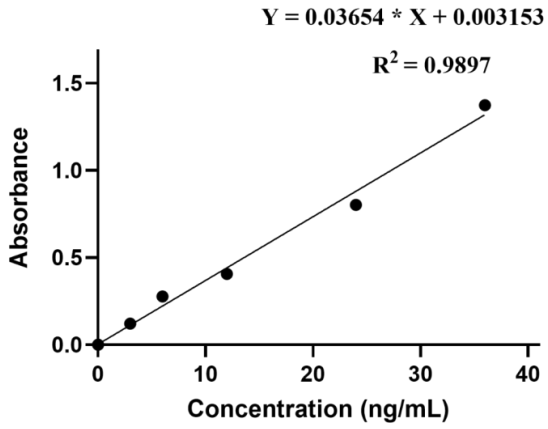

Figure 2. Standard curve for CYP450 quantification

Note: Absorbance values at 450 nm (y-axis) are plotted against known CYP450 standard concentrations (3, 6, 12, 24 and 36 ng/mL on x-axis). The dashed line represents the linear regression fit (Y=0.03654 ·X+0.003153; R^2=0.9897). The standard curve was used to interpolate CYP450 concentrations in liver homogenate samples in groups G3 and G4.

hepatic necrosis with leukocyte infiltration was also present (Figure 8D).

Kidney

Kidneys from the control group (G3) exhibited intact glomeruli and normal tubular architecture (Figure 9A). In contrast, kidneys from G4 showed granular RBC casts with tubular dilation (Figure 9B), tubular epithelial degeneration with ghost-like remnants (Figure 9C), acute tubular necrosis and degeneration with brick-red RBC casts (Figure 9D), extensive intratubular hemorrhage with congested blood vessels (Figures 9E and 9G), segmental glomerular atrophy, and intratubular hemorrhage with vascular congestion (Figure 9F).

Spleen

Histological examination of the spleen from the secondary control group (G3) showed normal architecture, with normal white and red spleen pulps (Figure 10A). In the secondary toxicity group (G4), the histopathological findings in spleen sections showed different degenerative lesions, such as white pulp atrophy with reduced

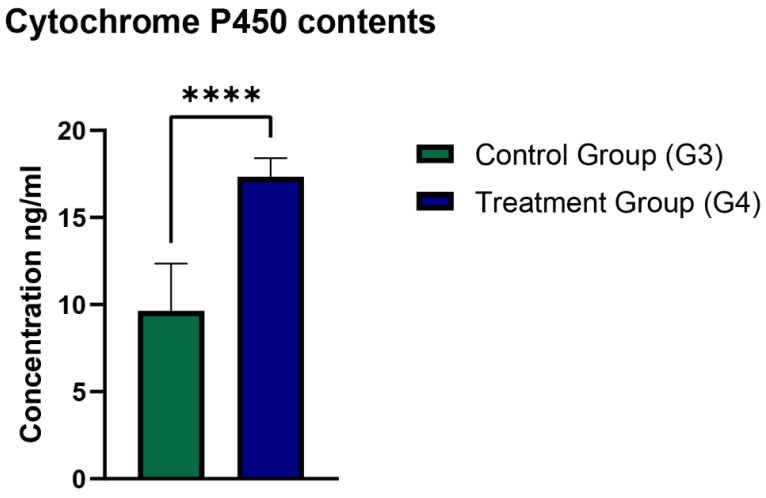

Figure 3. Hepatic cytochrome P450 concentrations in control (G3) and secondary toxicity (G4) groups following 4 weeks of exposure

****Significant difference at P<0.0001.

Note: Data are expressed as Mean±SD (n=12).

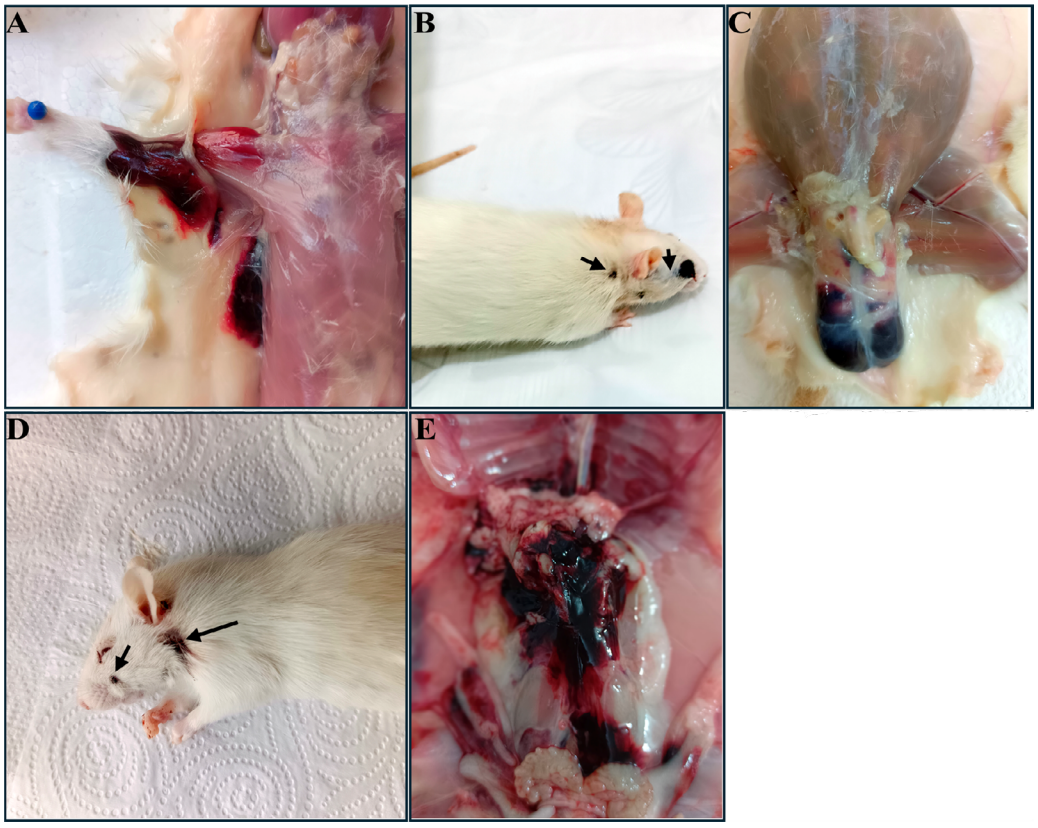

Figure 4. Gross pathological findings of hemorrhagic lesions in rats following lethal brodifacoum exposure

A) Gross pathological image of a rat in group G1 showing subcutaneous hemorrhage and muscular hematomas due to coagulopathy after lethal exposure to brodifacoum, B) Rats from group G1 showing external bleeding close to the eye and neck (arrows), C) Rat in group G1 showing severe testicular hemorrhage, D) Rats from group G1 showing external bleeding near the nose and neck (arrows), E) Rat in group G1 showing abdominal hemorrhage

lymphoid cells (Figure 10B), thinning of the marginal zone, and the absence of germinal centers (Figure 10C). Splenic red pulp lesions included aberrant and dilated sinusoidal structures, deposition of hemosiderin, increased trabeculae (Figure 10D), and lymphoid follicle depletion and necrosis (Figure 10F).

Lung

Lung sections from the control group (G3) displayed normal pulmonary parenchyma. Alveolar sacs were intact and uniformly expanded. Bronchioles and blood vessels maintained normal structural integrity, with no signs of congestion, hemorrhage, or alveolar edema (Figure 11A). Lung sections from G4 showed bronchiolar obstruction with necrotic debris, RBCs, and mucus exudate (Figure 11B). Vascular inflammation was evident, with lymphocytic infiltration (Figure 11C). Extensive inflammation disrupted lung architecture, with lymphoid follicles invading bronchiolar walls (Figure 11D). Bronchiolitis obliterans, alveolar wall thickening, and luminal obstruction were prominent (Figure 11E). Severe hemorrhage and inflammatory cell infiltration effaced alveolar and bronchiolar structures (Figure 11F), while alveolar septa exhibited hemorrhage and vascular congestion (Figure 11H).

Discussion

Brodifacoum exposure leads to several pathophysiological effects, primarily internal bleeding, by interfering with vitamin K recycling. The interference inhibits the activation of vitamin K-dependent clotting factors, which are essential for blood clotting and injury healing. CYP450 is the superfamily of enzymes primarily found in the liver and plays an important role in drug detoxification, cell metabolism, and homeostasis. The liver is also the main organ for brodifacoum accumulation, where it can persist for an extended period (Feinstein et al., 2016; Fisher, 2009; Rattner & Harvey, 2021). To our knowledge, no previous research has investigated the potential effect of brodifacoum on hepatic CYP450 levels. In this study, the total P450 levels were quantified and the results (Figure 3) demonstrated a significant 1.8-fold

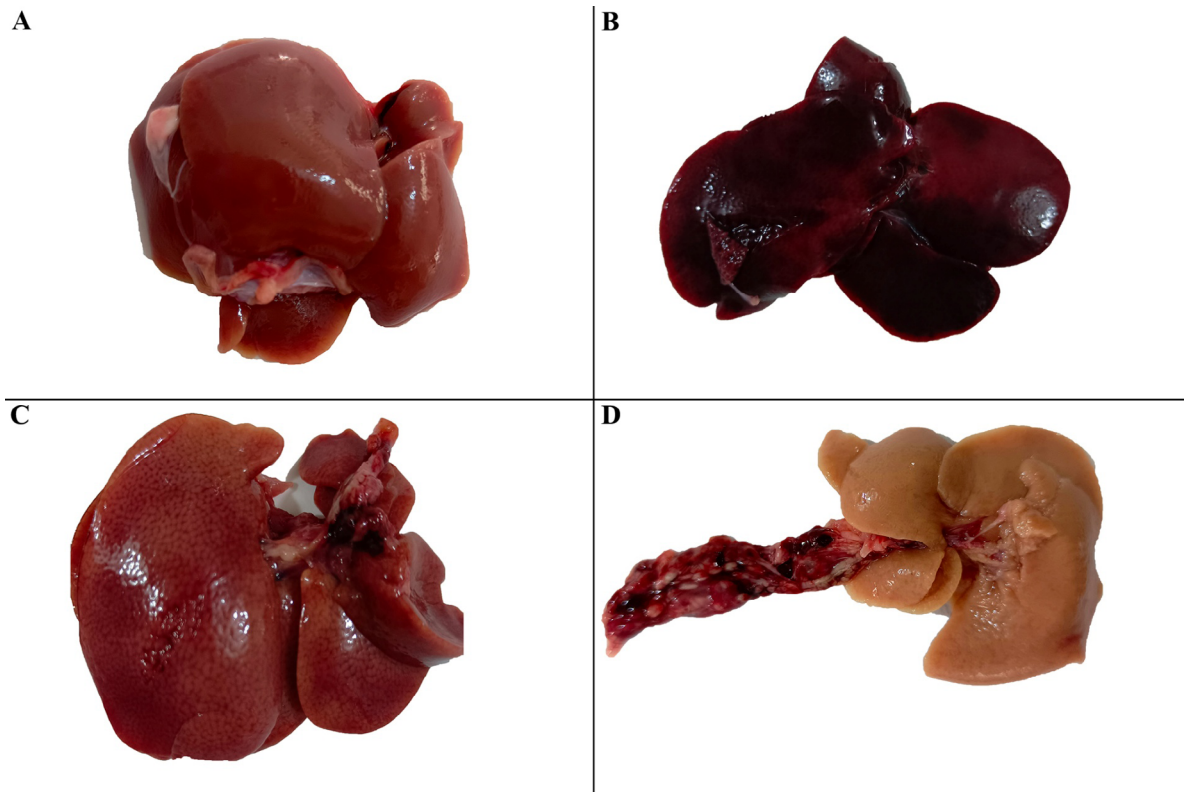

Figure 5. Gross pathological images of rats livers from in secondary control group (G3) and secondary toxicity group (G4) following 4 weeks of brodifacoum exposure

A) Normal liver architecture without any significant lesions, B) Severe congestion affecting multiple liver lobes, C) Edematous liver parenchyma with a rounded edge, D) Fatty liver and hepatomegaly

increase in G4, the secondary toxicity group, compared to G3, the secondary control group. The elevation of P450 in G4 indicates a liver response to the toxic effects of brodifacoum. Although this upregulation may suggest an attempt to enhance detoxification, it was insufficient to prevent brodifacoum-induced toxicity. CYP450 is composed of a number of isoforms, which are known to play important roles in the phase I metabolism of both xenobiotic and endobiotic compounds (Stading et al., 2020; Mohammed & Al-Shawi, 2025). Several studies have reported that an increase in p450 levels or the induction of certain CYP450 isoforms may increase cellular toxicity and cell injury (Cederbaum, 2010; Cui et al., 2025; Hameed & Hassan, 2022; Orellana & Guajardo, 2004). Although brodifacoum does not undergo significant metabolism in the liver, changes in CYP450 levels remain toxicologically relevant as the CYP450 enzyme family reflects environmental exposure and hepatic stress. Since biochemical subcellular alterations precede cellular and organism-level effects, P450 has been proposed as a sensitive biomarker and an early-warning system for assessing toxicant impact (Regnery et al., 2022; Rubinstein et al., 2019). It is plausible to conclude that the increase in total P450 is an adaptive hepatic response to oxidative or toxic stress rather than enzymatic induction. Several studies have suggested that the exposure to brodifacoum induces reactive oxygen species (ROS) production (Kalinin et al., 2017; Ware et al., 2015), which in turn has been associated with the upregulation of the expression of oxidative stress-responsive CYP isoforms, such as CYP2E1 and CYP1A1 (Jin et al., 2013; Stading et al., 2020; Ware et al., 2015). While our assay quantified total CYP450 rather than specific isoforms, this increase may indirectly reflect changes in these pathways. Furthermore, the activation of xenobiotic-sensing nuclear receptors, such as the pregnane X receptor (PXR) and the constitutive androstane receptor (CAR) might also contribute to this upregulation, and further research is needed to provide clarity in this context (Satoru et al., 2008; Yoshinari, 2019). Moreover, the oxidative potential of brodifacoum is not limited to the liver; earlier studies have demonstrated similar oxidative mechanisms contributing to brain and renal injury in rats (Kyle et al., 2015; Sergey et al., 2017). In this study, brodifacoum residues were quantified in rat livers from both primary and secondary exposure groups (G1 and G4, respectively). The mean liver concentration

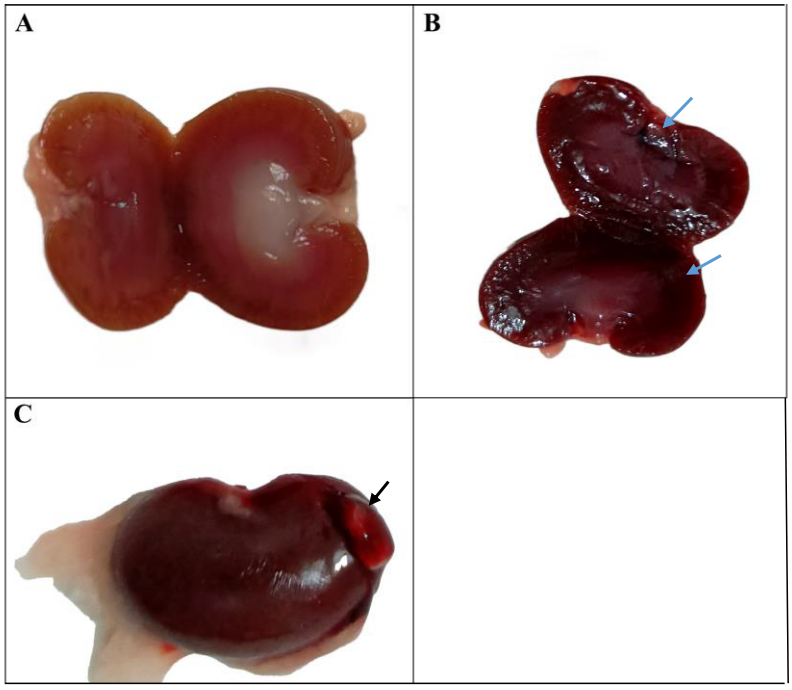

Figure 6. Gross pathological images of rat kidneys in the secondary control group (G3) and the secondary toxicity group (G4) following 4 weeks of brodifacoum exposure

A) Normal macroscopic appearance of a kidney in the secondary control group (G3), B) The cut surface of a G4 kidney showing multiple cortical and medullary hemorrhages (blue arrows), C) The kidney of a G4 rat is enlarged and exhibits a subcapsular hematoma (black arrow)

of brodifacoum in G1 was 3.53±0.49 µg/g, corresponding to liver residues from a single exposure to commercial bait containing 0.005% brodifacoum. These findings are comparable to those reported by Frankova et al. (2024), who used the same bait concentration in a no-choice feeding trial, and obtained comparable results: (3.16±1.34 µg/g) in the liver tissue. The secondary toxicity group (G4) that received 1 mL daily for 4 weeks of liver homogenate obtained from G1 showed a 5-fold higher liver concentration (17.87±0.11 µg/g) than the primary toxicity group (G1) (3.53±0.49 µg/g).

The high concentration of brodifacoum detected in the hepatic tissues of the secondary toxicity group (G4) (Table 2) is attributed to its tendency to accumulate in the liver tissue and its strong intracellular binding capac-

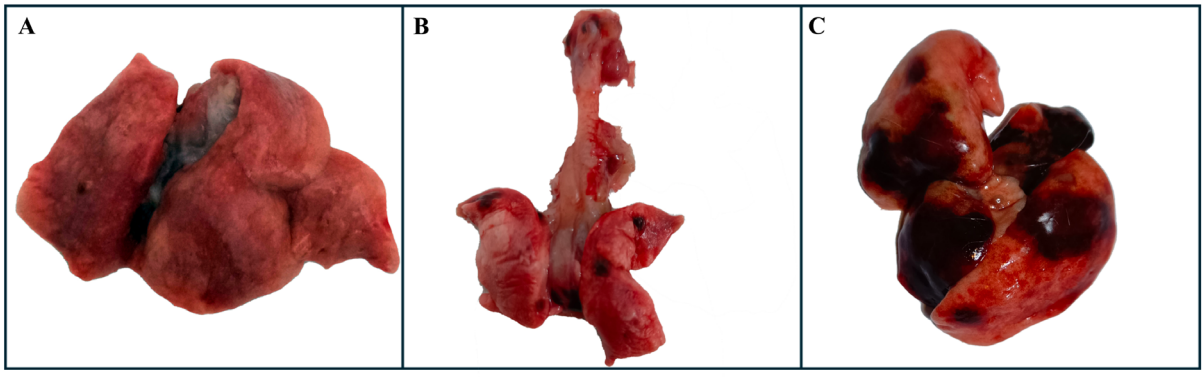

Figure 7. Gross pathological images of rats lungs in groups G3 and G4

A) Normal macroscopic appearance of lungs in the secondary control group (G3), B) The lungs in a G4 rat showing multiple hemorrhagic foci indicative of pulmonary hemorrhage and congestion, C) The lungs in a G4 rat exhibiting multifocal to coalescing dark red to black hemorrhagic patches involving multiple lobes (massive pulmonary hemorrhage)

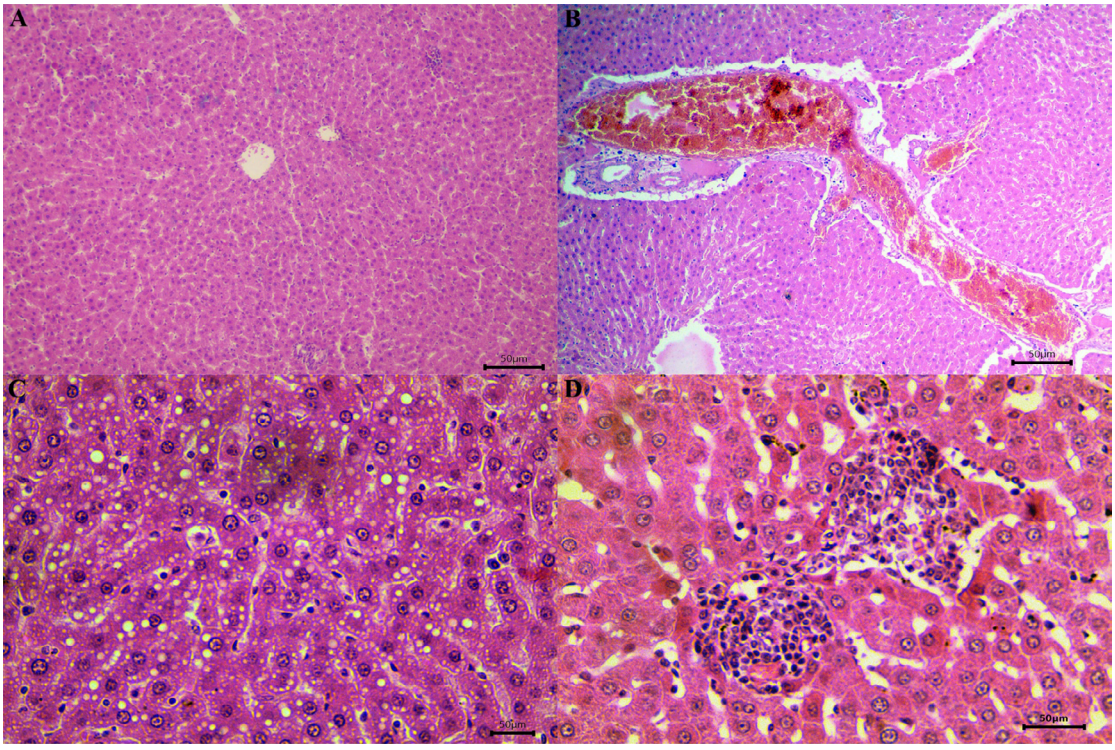

Figure 8. Histopathological findings of the liver in control (G3) and secondary toxicity (G4) groups

A) Histopathological section of the liver in a rat from group G3 (secondary control group) showing normal liver tissue (H&E, ×10), B) Histopathological section of the liver in a rat from group G4 (secondary toxicity group) showing extensive hemorrhage and edema occupying the portal area (H&E, ×20), C) The liver section in a rat from group G4 showing microvascular degeneration (H&E, ×40), D) The liver section in a rat from group G4 showing focal areas of hepatic necrosis with leucocytic cell infiltration (H&E, ×40)

ity following repeated exposure (Bachmann & Sullivan, 1983; Rattner et al., 2014). Furthermore, Frankova et al. (2024) reported that brodifacoum can accumulate to higher levels in the liver when rats ingest bait containing lower concentrations of brodifacoum, than when they ingest higher concentrations. It is worth noting that the delayed manifestation of brodifacoum toxicity in G4 compared to G1 suggests that brodifacoum sequestration in the liver may initially prevent toxicity until accumulation sites become saturated. Once saturated, free brodifacoum starts blocking a high proportion of vitamin K epoxide reductase (VKORC1) binding sites. Finally, the exhaustion of pre-existing clotting factors leads to bleeding. Moreover, the U.S. Environmental Protection Agency (EPA) noted that rodents exposed to SGARs, such as brodifacoum and difethialone, may continue to feed on baits and ingest doses ranging from 9 to 46 times the LD50, exceeding the minimum reported lethal threshold before succumbing (Hindmarch & Elliott, 2018). Collectively, this may explain the higher liver residue in the secondary toxicity group (G4) compared to the primary toxicity group, as well as the delayed manifestation of toxicity until the beginning of the third week. Monitoring liver residues in poisoned rats provides valuable insight into brodifacoum retention following secondary exposure in the experimental model (Fisher et al., 2004). It should be noted that the interpretation of liver residues is challenging, as it relates to past exposure and storage in the liver, not necessarily to the onset or severity of toxic effects (Rattner & Harvey, 2021).

Brodifacoum toxicity is mainly associated with excessive internal bleeding due to the vitamin K cycle disruption, the clinical manifestations of brodifacoum toxicity, such as lethargy, weakness, anorexia, dyspnea, reluctance to move, and ataxia, followed by death within 4–7 days. This delay is due to the time needed for the depletion of pre-existing K-dependent clotting factors, which usually takes between four and nine days. In our study, rats in the primary toxicity group (G1) that offered lethal brodifacoum bait showed signs of toxicity from 4 to 7 days after exposure. These findings are consistent with the typical finding at the organism level described in the literature (Rattner et al., 2014; Schmieg et al., 2025). Furthermore, rats in the secondary toxicity group (G4), which were administered liver homogenate from G1 animals, developed similar signs

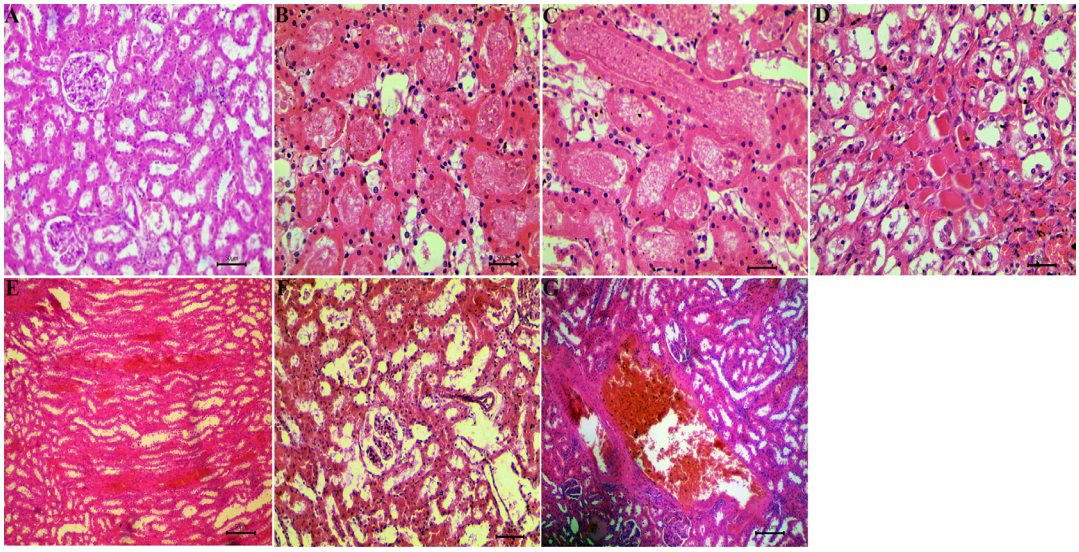

Figure 9. Histopathological findings of the kidney in control (G3) and secondary toxicity (G4) groups

A) Histopathological section of the kidney in a rat from group G3 (secondary control group) showing normal renal structure (H&E, ×20), B) Histopathological section of the kidney in a rat from group G4 (secondary toxicity group) showing an early stage of red blood cell casts within renal tubules; the majority of the casts are granular with massive tubular dilation (H&E, ×20), C) The kidney section in a rat from group G4 showing a spectrum of early stage of RBC casts, numerous ghost cells, and granular RBCs associated with dilation and degeneration of renal tubules (H&E, ×20); D) The kidney section in a rat from group G4 showing the late stage of RBC casts, where the majority of casts are compact and appear "brick-red" in color associated with acute tubular necrosis and degeneration (H&E, ×20), E) The kidney section in a rat from group G4 showing massive intratubular hemorrhage (H&E, ×20), F) The kidney section in a rat from group G4 showing glomerular atrophy and segmented glomeruli (H&E, ×20), G) The kidney section in a rat from group G4 showing extensive intratubular hemorrhage with congested blood vessels (H&E, ×40)

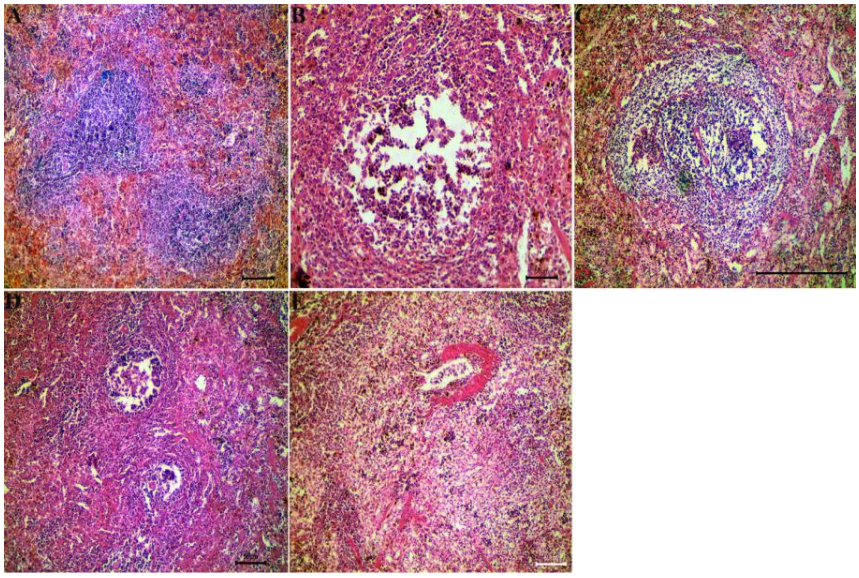

Figure 10. Histopathological findings of the spleen in control (G3) and secondary toxicity (G4) groups

A) Histopathological section of the spleen in a rat from group G3 (secondary control group) showing normal splenic tissue from the secondary control group G3, B) Histopathological section of the in a rat from group G4 (secondary toxicity group) showing splenic white pulp atrophy characterized by reduced lymphoid cells in the periarteriolar lymphoid sheath (H&E, ×20), C) The splenic section in a rat from group G4 showing a reduced white pulp area, a thinner marginal zone, and the absence of a germinal center (H&E, ×40), D) The splenic section in a rat from group G4 showing pathological alteration in the red pulp characterized by dilated sinusoids, hemosiderin deposits, and increased number of trabeculae (H&E, ×40), E) The splenic section in a rat from group G4 showing depletion of the white pulp with the absence of a germinal center and necrotic areas in the lymphoid follicle (H&E, ×40)

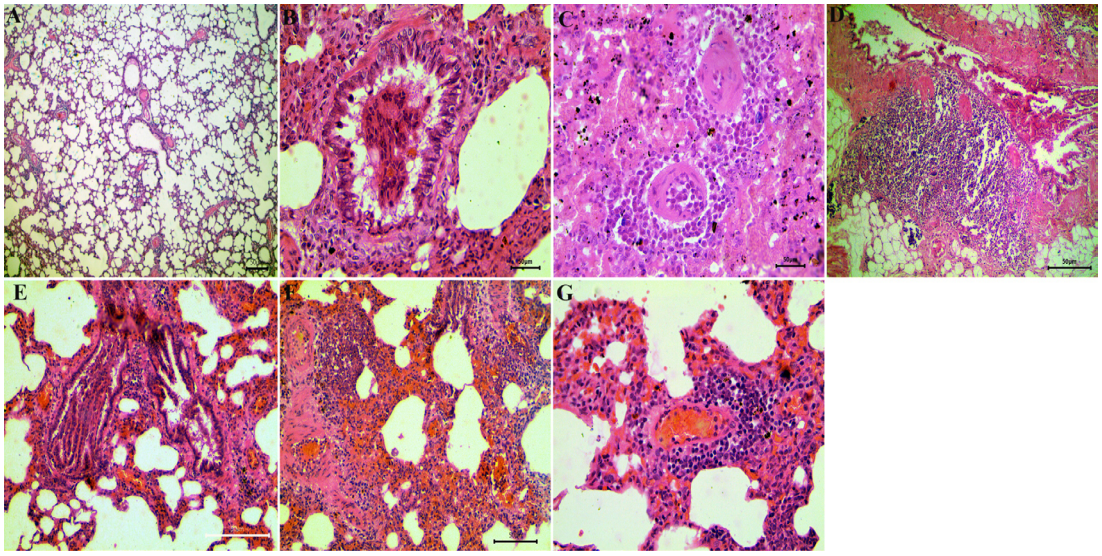

Figure 11. Histopathological findings of the lung in control (G3) and secondary toxicity (G4) groups

A) Histopathological section of the lung in a rat from group G3 (secondary control group) showing normal lung tissue (H&E, ×10); B) The lung section in a rat (secondary toxicity group) from group G4 showing bronchiole lumen obstruction with necrotic debris, RBCs, inflammatory cells, and mucous exudate (H&E, ×40); C) The lung section in a rat from group G4 showing that the lung architecture is obscured by inflammation: A large lymphoid follicle destroys the bronchiole wall and narrows its lumen (H&E, ×20); D) The lung section in a rat from group G4 showing bronchiolitis obliterans characterized by lumen obstruction associated with mucosal growth along the inner bronchiole wall. Alveolar walls are inflamed, thickened, discontinuous, and filled with RBCs and inflammatory cells (H&E, ×20); E) The lung section in a rat from group G4 showing that the lung architecture obscured by inflammation and hemorrhage. Alveolar and bronchiolar lumina are filled with abundant hemorrhage, RBCs, cellular debris (alveolar septal necrosis), and inflammatory cells that destroy bronchiolar walls and alveolar septa (H&E, ×20); F) The lung section in a rat from group G4 showing that alveolar septa are expanded by hemorrhage, inflammatory cells, and congested blood vessels (H&E, ×20); G) The lung section in a rat from group G4 showing alveolar septa filled with inflammatory cells, hemorrhage, accompanied by severe blood vessel (H&E, ×40)

similar to G1 but with more delayed onset, starting around the third week. The delayed signs in G4 reflect the time required for sufficient bioaccumulation of brodifacoum to reach threshold to impair vitamin K recycling and deplete functional clotting factors (Murray, 2011). In the present study, hemorrhagic lesions are the main finding based on gross organ examination, including the liver, kidney, and lung. Lungs had the highest hemorrhagic score (4) [3–4], followed by the liver (3) [2–4] and kidney (2) [2–3]. In contrast, another study reported the highest hemorrhagic score in the liver followed by kidney (Kaewamatawong et al., 2011). This finding emphasizes the high vascularity of the lung and its importance in the context of anticoagulation toxicity (Fitzgerald et al., 2018; Paulin et al., 2024). Moreover, the hemorrhage severity of the liver reflects the role of liver as the primary target organ for brodifacoum accumulation, which interferes with recycling of vitamin K1, resulting in the depletion of clotting factors eventually causing systemic bleeding. The importance of this finding lies in the fact that the coagulopathy observed across multiple organs in brodifacoum poisoning is fundamentally driven by liver injury. Therefore, hepatic lesions remain a key diagnostic indicator in suspected cases of anticoagulant rodenticide toxicity (Priya et al., 2025). In the histopathological context, secondary exposure in rats produced severe multisystemic histopathological changes, with lesions most evident in the liver, kidney, spleen, and lung. Our observation regarding changes in the liver tissue, such as extensive hemorrhage, marked dilatation, edema, vacuolations, focal infiltration, and aggregation of inflammatory cells are similar to the findings reported by other researchers (Atia et al., 2024; Gül et al., 2016). This vascular degeneration, hemorrhage, cellular injury, and dystrophic changes may result from the direct toxic effect of brodifacoum, in addition to indirect injury caused by anemia and hypoxia secondary to the disruption of hemostasis. Furthermore, the subsequent activation of inflammatory pathways and oxidative stress may exacerbate tissue damage and contribute to the progression and severity of these pathological changes (Popov Aleksandrov et al., 2024; Rattner et al., 2014). These degenerative changes, which suggest mitochondrial dysfunction and oxidative stress (Abbas & Jawad, 2023), are consistent with the indirect injury initiated by hypoxia. Meanwhile, the focal necrosis accompanied by leukocytic infiltration

reflects an inflammatory response to tissue damage (Hameed & Hassan, 2022). These results emphasize the role of the liver as a target organ for the accumulation and toxicity of brodifacoum (El-Daly & Nassar, 2014; Popov Aleksandrov et al., 2024). The renal alteration seen in the kidney of poisoned rats ranged from tubular degeneration and RBC casts to acute tubular necrosis and glomerular atrophy (Figure 9). These alterations resemble hemorrhagic nephropathy, previously reported in SGAR poisoning (Kalaitzidis et al., 2017). The severity of intratubular hemorrhage and vascular congestion and damage to glomerular and tubular epithelial cells could be explained by the nephrotoxic effect of brodifacoum on renal tubules (Binev et al., 2012). The prognoses of early granular casts to compact RBC casts indicates worsening tubular damage and suggests increased renal susceptibility to brodifacoum toxicity (Dvanajscak et al., 2020). Splenic white pulp atrophy, lymphoid follicle depletion, and hemosiderin deposition manifest both vascular injury and immunotoxicity. White pulp atrophy with absent germinal centers is consistent with the suppression of adaptive immunity, as noted in other SGAR cases (Öner & Gül, 2022; Rattner et al., 2014). Such immune impairment may increase the susceptibility to secondary infections subsequent to brodifacoum exposure (Kopanke et al., 2018). For example, brodifacoum exposure in rats has been shown to negatively affect the immune system, evidenced by the deterioration of the structure of CD4+ and CD8+ cells, suggesting functional immune impairment (Öner & Gül, 2022). Moreover, severe histopathological changes, such as bronchiolar obstruction with necrotic debris, alveolar hemorrhage, bronchiolitis obliterans, and vascular inflammation, were observed during the lung examination (Figure 11). Similar findings of widespread pulmonary congestion and hemorrhage have been reported in avian and mammals exposed to brodifacoum residues (Binev et al., 2012; Hughes et al., 2013; Popov Aleksandrov et al., 2024; Priya et al., 2025; Rattner et al., 2011). These pathological changes are secondary to brodifacoum-induced impairment of hemostasis. The clinical manifestation of such pathology may lead to respiratory distress in affected animals.

The toxicity of brodifacoum and other ARs are not limited to the acute exposure. Studies have shown that chronic or repeated exposure to sublethal doses can lead to adverse effects on the animal's overall health, influencing the ability of animal to cope with stressors, and increased susceptibility to diseases and infections, as noted by Rattner et al. (2014).

Conclusion

This study demonstrated that consuming the liver homogenate contaminated with brodifacoum can induce secondary toxicity in rats. HPLC analysis confirmed marked hepatic accumulation, and ELISA results showed increased CYP450 activity. These finding were accompanied by notable gross and histopathological hemorrhagic and degenerative lesions in major organs, including the liver, kidneys, lungs, and spleen. These findings provide controlled laboratory evidence of secondary brodifacoum toxicity in a mammalian model and strengthen the understanding of toxic responses following indirect exposure. Further work involving models that better represent natural feeding interactions would enhance the evaluation of secondary exposure risks in broader biological contexts.

Study limitation

An inherent limitation of the experimental design of this study is the use of an intraspecific model (rat-to-rat consumption) to investigate secondary exposure. While this design offers a controlled, practical, and ethically acceptable system for investigating secondary exposure, its findings cannot be directly extrapolated to the complex interspecific dynamics of natural food webs. Predators and scavengers in the nature encompass a wide range of avian and mammalian species, each with unique metabolic rates, feeding behaviors, and sensitivities to anticoagulants.

Ethical Considerations

Compliance with ethical guidelines

This study was approved by the Ethics Committee of the College of Veterinary Medicine, University of Baghdad, Baghdad, Iraq (Code: P.G/1282 on 26/5/2025).

Funding

This study was extracted from the master's thesis of Mohammed A Mahdi Al-Kubaisi, approved by the Department of Animal Pathology and Poultry Diseases, College of Veterinary Medicine, University of Baghdad, Baghdad, Iraq.

Authors' contributions

All authors contributed equally to the conception and design of the study, data collection and analysis, interception of the results and drafting of the manuscript. Each author approved the final version of the manuscript for submission.

Conflict of interest

The authors declared no conflict of interest.

Acknowledgments

The authors thank the College of Veterinary Medicine, University of Baghdad, for providing the resources and facilities necessary to carry out this work.

References

Abbas, M. I., & Jawad, Z. J. (2023). Hepatoprotective effect of alcoholic extract of ficus carica leaves against cypermethrin-induced liver toxicity in male albino rats. *The Iraqi Journal of Veterinary Medicine, 47*(2), 64-72. [DOI:10.30539/ijvm.v47i2.1601]

Abduljalel, M. E., & Al-Saadi, R. N. (2022). Toxicopathological effect of benzene, toluene, ethylbenzene, and xylenes (btex) as a mixture and the protective effect of citicoline in male rats followings 90-day oral exposure. *REDVET-Revista Electrónica de Veterinaria, 23*(3), 399 - 414. [Link]

Al-Saadi, R., Mohammed Jawad, Z. J., Khalaf, O. H., & Muhsain, S. N. F. (2025). Histopathological effects of repeated 14-day administration of rizatriptan benzoate in a nitroglycerin-induced migraine rabbits model. *Open Veterinary Journal, 15*(1), 179–186. [DOI:10.5455/ovj.2025.v15.i1.17] [PMID]

Ammar, H. S., & Mohammed Mosleh, S. (2024). Green synthesis, lead toxicity and pharmacokinetic evaluation of sumac silver nanoparticles in vivo. *Journal of Angiotherapy, 8*(4), 1-6. [Link]

Atia, M. M., Mahmoud, H. A. A., Wilson, M., & Abd-Allah, E. A. (2024). A comprehensive survey of warfarin-induced hepatic toxicity using histopathological, biomarker, and molecular evaluation. *Heliyon, 10*(4), e26484. [DOI:10.1016/j.heliyon.2024.e26484] [PMID]

Bachmann, K. A., & Sullivan, T. J. (1983). Dispositional and pharmacodynamic characteristics of brodifacoum in warfarin-sensitive rats. *Pharmacology, 27*(5), 281-288. [DOI:10.1159/000137881] [PMID]

Binev, R., Valchev, I., Groseva, N., Lazarov, L., Hristov, T., & Uzunova, K. (2012). Morphological investigations of experimental acute intoxication with the anticoagulant rodenticide bromadiolone in pheasants. *İstanbul Üniversitesi Veteriner Fakültesi Dergisi, 38*(2), 161-173. [Link]

Buckley, J. Y., Needle, D. B., Royar, K., Cottrell, W., Tate, P., & Whittier, C. (2023). High prevalence of anticoagulant rodenticide exposure in New England Fishers (Pekania pennanti). *Environmental Monitoring and Assessment, 195*(11), 1348. [DOI:10.1007/s10661-023-11919-x] [PMID]

Caliani, I., Di Noi, A., Amico, C., Berni, R., Romi, M., & Cai, G., et al. (2023). Brodifacoum Levels and Biomarkers in Coastal Fish Species following a Rodent Eradication in an Italian Marine Protected Area: Preliminary Results. *Life (Basel, Switzerland), 13*(2), 415. [DOI:10.3390/life13020415][PMID]

Cederbaum A. I. (2010). Role of CYP2E1 in ethanol-induced oxidant stress, fatty liver and hepatotoxicity. *Digestive Diseases (Basel, Switzerland), 28*(6), 802–811. [DOI:10.1159/000324289] [PMID]

Cui, R., Pan, A., Wang, T., Liang, Y., & Yu, H. F. (2025). Aflatoxin b1 in animals: Metabolism and immunotoxicity. *The Pakistan Veterinary Journal, 45*(3), 923-934. [DOI:10.29261/pakvetj/2025.207]

Dvanajscak, Z., Cossey, L. N., & Larsen, C. P. (2020). A practical approach to the pathology of renal intratubular casts. *Seminars in Diagnostic Pathology, 37*(3), 127-134. [DOI:10.1053/j.semdp.2020.02.001] [PMID]

El-Daly, A. A., & Nassar, S. A. (2014). Anticoagulant difenacoum-induced histological and ultrastructural alterations in liver of albino rats. *International Journal of Advanced Research, 2*, 782-792. [Link]

Feinstein, D. L., Akpa, B. S., Ayee, M. A., Boullerne, A. I., Braun, D., & Brodsky, S. V., et al. (2016). The emerging threat of superwarfarins: history, detection, mechanisms, and countermeasures. *Annals of the New York Academy of Sciences, 1374*(1), 111–122. [DOI:10.1111/nyas.13085] [PMID]

Fisher, P. M. (2009). Residual concentrations and persistence of the anticoagulant rodenticides brodifacoum and diphacinone in fauna [PhD dissertation]. Lincoln: Lincoln University. [Link]

Fisher, P., O'Connor, C., Wright, G., & Eason, C. (2004). *Anticoagulant residues in rats and secondary non-target risk.* Wellington, New Zealand: Department of Conservation. [Link]

Fitzgerald, S. D., Martinez, J., & Buchweitz, J. P. (2018). An apparent case of brodifacoum toxicosis in a whelping dog. *Journal of Veterinary Diagnostic Investigation : Official Publication of the American Association of Veterinary Laboratory Diagnosticians, Inc, 30*(1), 169–171. [DOI:10.1177/1040638717741664] [PMID]

Frankova, M., Radostna, T., Aulicky, R., & Stejskal, V. (2024). Less brodifacoum in baits results in greater accumulation in the liver of captive rattus norvegicus in a no-choice trail. *Journal of Pest Science, 97*(4), 2273-2280. [DOI:10.1007/s10340-023-01737-y]

Gül, N., Yiğit, N., Saygılı, F., Demirel, E., & Geniş, C. (2016). Comparison of the effects of difenacoum and brodifacoum on the ultrastructure of rat liver cells. *Arhiv Za Higijenu Rada i Toksikologiju, 67*(3), 204–209. [DOI:10.1515/aiht-2016-67-2783] [PMID]

Hameed, H. A., & Hassan, A. F. (2022). The prophylactic anti-inflammatory effect of omega-7 against paracetamol-induced liver injury in rats. *The Iraqi Journal of Veterinary Medicine, 46*(2), 43-47. [DOI:10.30539/ijvm.v46i2.1412]

Hernández-Moreno, D., Irene de la Casa, R., López-Beceiro, A. M., Fidalgo, L. E., Soler, F. D., & Pérez-López, M. (2013). Secondary poisoning of non-target animals in an ornithological zoo in galicia (nw spain) with anticoagulant rodenticides: A case report. *Veterinární Medicína, 58*(10), 553-559. [DOI:10.17221/7087-VETMED]

Hindmarch, S., & Elliott, J. E. (2018). Ecological factors driving uptake of anticoagulant rodenticides in predators. In N. W. van den Brink, J. E. Elliott, R. F. Shore, & B. A. Rattner (Eds.), *Anticoagulant rodenticides and wildlife* (pp. 229-258). Cham: Springer International Publishing. [DOI:10.1007/978-3-319-64377-9_9]

Hughes, J., Sharp, E., Taylor, M. J., Melton, L., & Hartley, G. (2013). Monitoring agricultural rodenticide use and secondary exposure of raptors in Scotland. *Ecotoxicology (London,*

England), 22(6), 974–984. [DOI:10.1007/s10646-013-1074-9] [PMID]

Jin, M., Ande, A., Kumar, A., & Kumar, S. (2013). Regulation of cytochrome P450 2e1 expression by ethanol: Role of oxidative stress-mediated pkc/jnk/sp1 pathway. *Cell Death & Disease, 4*(3), e554. [PMID] [DOI:10.1038/cddis.2013.78]

Kaewamatawong, T., Lohavanijaya, A., Charoenlertkul, P., & Srichairat, S. (2011). Retrospective histopathological study of hemorrhagic lesion of coumarin intoxication in dogs. *The Thai Journal of Veterinary Medicine, 41*(2), 239-244. [DOI:10.56808/2985-1130.2302]

Kalaitzidis, R. G., Duni, A., Liapis, G., Balafa, O., Xiromeriti, S., & Rapsomanikis, P. K., et al. (2017). Anticoagulant-related nephropathy: A case report and review of the literature of an increasingly recognized entity. *International Urology and Nephrology, 49*(8), 1401–1407. [DOI:10.1007/s11255-017-1527-9] [PMID]

Kalinin, S., Marangoni, N., Kowal, K., Dey, A., Lis, K., & Brodsky, S., et al. (2017). The Long-Lasting Rodenticide Brodifacoum Induces Neuropathology in Adult Male Rats. *Toxicological Sciences : An Official Journal of the Society of Toxicology, 159*(1), 224–237. [DOI:10.1093/toxsci/kfx134] [PMID]

King, N., & Tran, M. H. (2015). Long-acting anticoagulant rodenticide (superwarfarin) poisoning: A review of its historical development, epidemiology, and clinical management. *Transfusion Medicine Reviews, 29*(4), 250-258. [DOI:10.1016/j.tmrv.2015.06.002] [PMID]

Kopanke, J. H., Horak, K. E., Musselman, E., Miller, C. A., Bennett, K., & Olver, C. S., et al. (2018). Effects of Low-level Brodifacoum Exposure on the Feline Immune Response. *Scientific Reports, 8*(1), 8168. [DOI:10.1038/s41598-018-26558-3] [PMID]

Kyle, W., Douglas, L. F., Israel, R., Guy, L. W., Brad, H. R., & Lee, A. H., et al. (2015). Brodifacoum induces early hemoglobinuria and late hematuria in rats: Novel rapid biomarkers of poisoning. *American Journal of Nephrology, 41*(4-5), 392-399. [DOI:10.1159/000433568] [PMID]

Meiser, H. (2005). Detection of anticoagulant residues by a new hplc method in specimens of poisoned animals and a poison control case study. *Journal of Analytical Toxicology, 29*(6), 556-563. [DOI:10.1093/jat/29.6.556] [PMID]

Mohammed, R. A., & Al-Shawi, N. N. (2025). Butein mitigates 5-FU-triggered hepatotoxicity via antioxidant, anti-inflammatory, and anti-apoptotic pathways. *Toxicology Reports, 15*, 102120. [DOI:10.1016/j.toxrep.2025.102120] [PMID]

Murray, M. (2011). Anticoagulant rodenticide exposure and toxicosis in four species of birds of prey presented to a wildlife clinic in massachusetts, 2006–2010. *Journal of Zoo and Wildlife Medicine, 42*(1), 88-97. [DOI:10.1638/2010-0188.1] [PMID]

Murray, M. (2020). Continued anticoagulant rodenticide exposure of red-tailed hawks (buteo jamaicensis) in the northeastern united states with an evaluation of serum for biomonitoring. *Environmental Toxicology and Chemistry, 39*(11), 2325-2335. [DOI:10.1002/etc.4853] [PMID]

Mustafa, M. Q., & Jawad, Z. J. (2024). Evaluating the hepatoprotective potential of ginger ethanolic extract against lambda-cyhalothrin-induced toxicity in male rats. *The Iraqi Journal of Veterinary Medicine, 48*(2), 26-31. [DOI:10.30539/r5qyq534]

Öner, B. B., & Gül, N. (2022). Histochemical effects of brodifacoum on rat spleen. Communications *Faculty of Sciences University of Ankara Series C Biology, 31*(2), 148-164. [DOI:10.53447/communc.1168968]

Orellana, M., & Guajardo, V. (2004). Actividad del citocromo P450 y su alteración en diversas patologías [Cytochrome P450 activity and its alteration in different diseases (Spanish)]. *Revista Medica de Chile, 132*(1), 85–94. [DOI:10.4067/s0034-98872004000100014] [PMID]

Paulin, M. V., Bray, S., Laudhittirut, T., Paulin, J., Blakley, B., & Snead, E. (2024). Anticoagulant rodenticide toxicity in dogs: A retrospective study of 349 confirmed cases in Saskatchewan. *The Canadian Veterinary Journal = La Revue Veterinaire Canadienne, 65*(5), 496–503. [PMID]

Popov Aleksandrov, A., Tucovic, D., Kulas, J., Popovic, D., Kataranovski, D., & Kataranovski, M., et al. (2024). Toxicology of chemical biocides: Anticoagulant rodenticides - Beyond hemostasis disturbance. Comparative biochemistry and physiology. *Toxicology & Pharmacology : CBP, 277*, 109841. [DOI:10.1016/j.cbpc.2024.109841] [PMID]

Priya, P. N., Pechimuthu, J., Palaniappan, V., Boopathy, T., Anbazhagan, J., & Muniraj, J. (2025). Histomorphological study of rodenticide poisoning: An autopsy-based cross-sectional study from a tertiary care centre, krishnagiri, tamil nadu, india. *Journal of Clinical & Diagnostic Research, 19*(1), EC17 - EC21. [DOI:10.7860/JCDR/2025/74981.20558]

Rached, A., Moriceau, M. A., Serfaty, X., Lefebvre, S., & Lattard, V. (2020). Biomarkers Potency to Monitor Non-target Fauna Poisoning by Anticoagulant Rodenticides. *Frontiers in Veterinary Science, 7*, 616276. [DOI:10.3389/fvets.2020.616276] [PMID]

Ragab, S., Sayed, Z., Sayed, S., Omar, H., & Omar, M. (2019). Effects of brodifacoum, acetylsalicylic acid and its combination on haemostatic, hematological and hepatic markers of wild rat rattus rattus. *Assiut University Journal of Zoology, 48*(2), 60-86. [Link]

Rattner, B. A., & Harvey, J. J. (2021). Challenges in the interpretation of anticoagulant rodenticide residues and toxicity in predatory and scavenging birds. *Pest Management Science, 77*(2), 604–610. [DOI:10.1002/ps.6137] [PMID]

Rattner, B. A., & Mastrota, F. N. (2018). Anticoagulant rodenticide toxicity to non-target wildlife under controlled exposure conditions. In N. van den Brink, J. Elliott, R. Shore & B. Rattner (Eds), *Anticoagulant Rodenticides and Wildlife. Emerging Topics in Ecotoxicology, vol 5.* Cham: Springer. [DOI:10.1007/978-3-319-64377-9_3]

Rattner, B. A., Horak, K. E., Warner, S. E., Day, D. D., Meteyer, C. U., & Volker, S. F., et al. (2011). Acute toxicity, histopathology, and coagulopathy in American kestrels (Falco sparverius) following administration of the rodenticide diphacinone. *Environmental Toxicology and Chemistry, 30*(5), 1213–1222. [DOI:10.1002/etc.490] [PMID]

Rattner, B. A., Lazarus, R. S., Elliott, J. E., Shore, R. F., & van den Brink, N. (2014). Adverse outcome pathway and risks of anticoagulant rodenticides to predatory wildlife. *Environmental Science & Technology, 48*(15), 8433-8445. [DOI:10.1021/es501740n] [PMID]

Rattner, B. A., Volker, S. F., Lankton, J. S., Bean, T. G., Lazarus, R. S., & Horak, K. E. (2020). Brodifacoum Toxicity in American Kestrels (Falco sparverius) with Evidence of Increased Hazard on Subsequent Anticoagulant Rodenticide Exposure. *Environmental Toxicology and Chemistry, 39*(2), 468–481. [DOI:10.1002/etc.4629] [PMID]

Regnery, J., Riegraf, C., Jacob, S., & Friesen, A. (2022). New insights on in vitro biotransformation of anticoagulant rodenticides in fish. *Chemosphere, 294,* 133727. [DOI:10.1016/j.chemosphere.2022.133727] [PMID]

Riegraf, C., Olbrich, D., & Vermeirssen, E. (2022). *Anticoagulant rodenticides – Swiss situation analysis.* Dübendorf, Switzerland: Swiss Centre for Applied Ecotoxicology. [Link]

Rubinstein, I., van Breemen, R., Nosal, D. G., Weinberg, G., Hershow, R. C., & Feinstein, D. L. (2019). Should Cytochrome P450 Inducers be Used to Accelerate Clearance of Brodifacoum from Poisoned Patients?. *Drugs in R&D, 19*(1), 67–71. [DOI:10.1007/s40268-019-0261-4] [PMID]

Satoru, K., Yuichi, Y., Daichi, T., & Masahiko, N. (2008). New insights on the xenobiotic-sensing nuclear receptors in liver diseases – car and pxr. *Current Drug Metabolism, 9*(7), 614-621. [DOI:10.2174/138920008785821666] [PMID]

Scammell, K., Cooke, R., Yokochi, K., Carter, N., Nguyen, H., & White, J. G. (2024). The missing toxic link: Exposure of non-target native marsupials to second-generation anticoagulant rodenticides (sgars) suggest a potential route of transfer into apex predators. *The Science of The Total Environment, 933,* 173191. [DOI:10.1016/j.scitotenv.2024.173191] [PMID]

Schmieg, H., Ferling, H., Bucher, K. A., Jacob, S., Regnery, J., & Schrader, H., et al. (2025). Brodifacoum causes coagulopathy, hemorrhages, and mortality in rainbow trout (oncorhynchus mykiss) at environmentally relevant hepatic residue concentrations. *Ecotoxicology and Environmental Safety, 289,* 117629. [DOI:10.1016/j.ecoenv.2024.117629] [PMID]

Kalinin, S., Marangoni, N., Kowal, K., Dey, A., Lis, K., & Brodsky, S., et al. (2017). The Long-Lasting Rodenticide Brodifacoum Induces Neuropathology in Adult Male Rats. *Toxicological Sciences : An Official Journal of the Society of Toxicology, 159*(1), 224–237. [DOI:10.1093/toxsci/kfx134] [PMID]

Shahwar, D. E., Azeem, S. A., Kawan, A., Mukhtar, H., Sajawal, A., & Noureen, S., et al. (2024). Significance of additives to enhance the acceptance of poison bait in poultry rodents of Haripur, Khyber Pakhtunkhwa, Pakistan. *Plos One, 19*(1), e0272397. [PMID]

Shakir, Z., & Al-Saadi, R. (2025). Exposure to environmental perfluorooctanoic acid (pfoa) induced hepatocellular apoptosis and alteration in serum biomarkers in diabetic guinea pigs. *Advances in Animal and Veterinary Sciences, 13*(5), 1097-1103. [DOI:10.17582/journal.aavs/2025/13.5.1097.1103]

Soh, S., Chua, C., Griffiths, J., Oh, P., Chow, J., & Chan, Q., et al. (2022). The use of anticoagulants for rodent control in a mixed-use urban environmefent in Singapore: A controlled interrupted time series analysis. *Plos One, 17*(5), e0267789. [DOI:10.1371/journal.pone.0267789] [PMID]

Stading, R., Chu, C., Couroucli, X., Lingappan, K., & Moorthy, B. (2020). Molecular role of cytochrome P4501A enzymes in oxidative stress. *Current Opinion in Toxicology, 20-21,* 77–84. [DOI:10.1016/j.cotox.2020.07.001] [PMID]

Valverde, I., Espín, S., Gómez-Ramírez, P., Navas, I., María-Mojica, P., & Sánchez-Virosta, P., et al. (2021). Wildlife poisoning: A novel scoring system and review of analytical methods for anticoagulant rodenticide determination. *Ecotoxicology, 30*(5), 767-782. [DOI:10.1007/s10646-021-02411-8] [PMID]

Ware, K. M., Feinstein, D. L., Rubinstein, I., Weinberg, G., Rovin, B. H., & Hebert, L., et al. (2015). Brodifacoum induces early hemoglobinuria and late hematuria in rats: novel rapid biomarkers of poisoning. *American Journal of Nephrology, 41*(4-5), 392–399. [DOI:10.1159/000433568] [PMID]

Ware, K. M., Feinstein, D. L., Rubinstein, I., Battula, P., Otero, J., & Hebert, L., et al. (2017). The Severity of Intracranial Hemorrhages Measured by Free Hemoglobin in the Brain Depends on the Anticoagulant Class: Experimental Data. *Stroke Research and Treatment, 2017,* 6516401. [DOI:10.1155/2017/6516401] [PMID]

Yoshinari K. (2019). Role of Nuclear Receptors PXR and CAR in Xenobiotic-Induced Hepatocyte Proliferation and Chemical Carcinogenesis. *Biological & Pharmaceutical Bulletin, 42*(8), 1243–1252. [DOI:10.1248/bpb.b19-00267] [PMID]

This Page Intentionally Left Blank